Theor Chem Acc (2011) 128:695–703
DOI 10.1007/s00214-010-0769-8

REGULAR ARTICLE

Influence of the sodium and calcium non-framework cations on the adsorption of hexane isomers in zeolite BEA

Elena García-Pérez · Patrick S. Barcia · José A. C. Silva · Alirio E. Rodrigues · Sofía Calero

Received: 8 April 2010 / Accepted: 17 May 2010 / Published online: 10 June 2010

Abstract We have performed configurational-bias Monte Carlo simulations to compute pure component adsorption isotherms of *n*-hexane, 3-methylpentane and 2,2-dimethylbutane in BEA-Polymorphs A and B at 423 K. The effect of the density and nature of influence of non-framework cations was systematically analyzed. Our results show that differences in the type and concentration of the non-framework cations lead to differences in adsorption loading. We found that this behavior is directly related to the preferential adsorption sites of the isomers as well as to the amount and location of the non-framework cations.

Keywords Zeolites · Adsorption · Simulations · Monte Carlo method

Published as part of the special issue celebrating theoretical and computational chemistry in Spain.

E. García-Pérez · S. Calero (✉)
Department of Physical, Chemical, and Natural Systems, University Pablo de Olavide, Ctra. Utrera km. 1, 41013 Seville, Spain
e-mail: scalero@upo.es

P. S. Barcia · J. A. C. Silva
Escola Superior de Tecnologia e Gestão, Instituto Politécnico de Bragança, 5301-857 Bragança, Portugal

P. S. Barcia · A. E. Rodrigues
Laboratory of Separation and Reaction Engineering, Departamento de Engenharia Química, Faculdade de Engenharia, Universidade do Porto, Rua do Dr. Roberto Frias, S/N, 4200-465 Porto, Portugal

1 Introduction

Zeolite beta, also called BEA, was first synthesized by Mobil Oil Corporation in 1967 [1]. It consists of 3D interconnecting channels with 12-membered rings. The pore diameters of the structure are approximately 6.6 × 6.7 Å (linear channels) and 5.6 × 5.6 Å (sinusoidal channels), which is similar to other large-pore molecular sieves such as FAU-type zeolites. One of the special features of zeolite BEA is its high level of disorder. This disorder appears because of the coexistence of two related structures [2, 3], polymorph A (enantiomorphic $P4_122$ or $P4_322$) and polymorph B (monoclinic symmetry C_2/c), with multiple internal structure defects.

Zeolite BEA shows acidic and catalytic properties and high hydrocarbon adsorption capacity under extreme conditions. In spite of its popularity in petrochemical industries, not many data relating to the adsorption and diffusion of alkanes in this zeolite are published. Some publications describe experimental studies on separation of hexane isomers in H-beta [4–6] and Ba-beta [4, 5], on adsorption of toluene [7, 8], benzene [9] and propene [7] on BEA with different amount of aluminum framework atoms per unit cell, and on the separation of N_2, O_2, CO_2 and CH_4 on BEA [10]. Lu et al. [11] report simulated data on BEA, studying the separation of butane isomers in pure silica BEA, and some results from Liu et al. [12] that compared the adsorption isotherms of C_1–C_7 linear alkanes on BEA with MFI and MOR-type zeolites.

In a previous study, Barcia et al. analyzed simultaneous adsorption energies of C_6 isomers in BEA. They provided experimental data for the pure components, fitted the data to a tri-site Langmuir model and formulated a multicomponent Langmuir model to predict mixture adsorption energy behavior [6]. The authors also discussed the

existence of a third active site for adsorption at the intersections between zig–zag and straight channels in addition to those along the two types of channels. In this work, we present a computational study to analyze the adsorption behavior of *n*-hexane (nHex), 3-methylpentane (3MP) and 2,2-dimethylbutane (22DMB) in the two polymorphs of BEA. The aim of this work is twofold: first to analyze the effect of the amount of aluminum framework atoms per

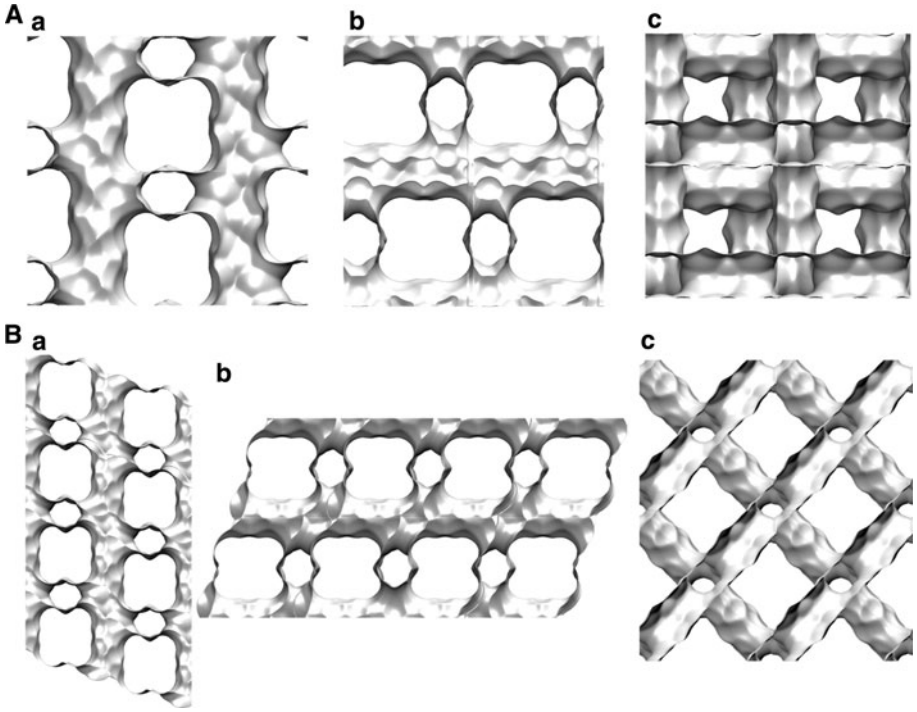

Fig. 1 Equipotential energy profiles for polymorph **A** (*top*), along the *a* (*left*), *b* (*medium*) and *c* (*right*) projection; and polymorph **B** (*bottom*) along the *a* (*left*), *b* (*medium*), both rotated by 45 degrees to obtain a view along the channels, and *c* (*right*) projection

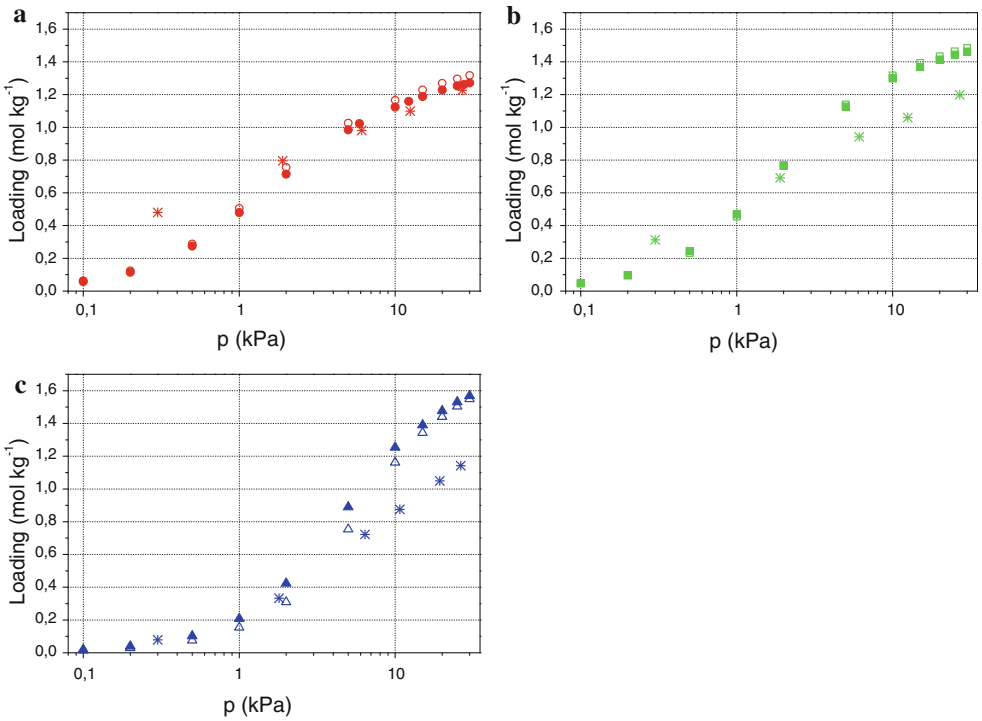

Fig. 2 Computed adsorption isotherms of hexane (*top left*), 3-methylpentane (*top right*) and 2,2-dimethylbutane (*bottom*) in pure silica polymorph A (*open symbols*) and polymorph B (*solid symbols*) at 423 K. Experimental isotherms for BEA (*asterisks*) are included for comparison

unit cell and the effect of the type of non-framework cations on the hydrocarbon adsorption and second to identify the preferential adsorption sites in BEA as a function of pressure, number of aluminum atoms and type of cation. In Sect. 2, we present our simulation methods. We continue in Sect. 3 with simulation results. These include adsorption isotherms and studies on preferential adsorption sites. Section 4 contains concluding remarks.

2 Simulation methods

Zeolite beta is a hybrid of two intergrowing polymorphs. Polymorph A has space group $P4_122$ or $P4_322$, while polymorph B has $C2/c$. In both polymorphs, the 12-membered rings pore system is three-dimensional, with two straight channels, each with a cross-section of approximately 6.6 × 6.7 Å, parallel to the [1 0 0] and [0 1 0] directions and a tortuous channel of 5.6 × 5.6 Å along the [0 0 1] direction. The latter is formed by the intersections of the two linear channel systems.

The adsorption isotherms for *n*-hexane, 3-methylpentane and 2,2-dimethylbutane in BEA, polymorphs A and B, were calculated using the configurational-bias Monte Carlo (CBMC) method in the grand canonical (GC) ensemble where temperature T, volume V and fugacity f remained constant. The crystallographic data of the structure are available elsewhere [13]. The two BEA-polymorph frameworks consist of silicon, aluminum and oxygen atoms (a total of 192 atoms per unit cell). The structures are assumed rigid during simulations, with static atomic charges $q_{Si} = +2.05$, $q_{Al} = +1.75$, $q_O = -1.025$ (bridging two silicon atoms), $q_{Oa} = -1.2$ (bridging one silicon and one aluminum atom), $q_{Na} = +1.0$ and $q_{Ca} = +2.0$, following our previous work [14–19]. Structures with aluminum were obtained by randomly replacing silicon by aluminum atoms, satisfying the Löwenstein rule, which forbids Al–O–Al linkages. The total number of cations remains constant during simulations. The cations are allowed to move freely in the structure using random displacements. The hydrocarbon molecules are described with a united atom TraPPE model [20], in which CH_3, CH_2, CH and C beads are treated as single interaction centers. The beads are connected using a harmonic bond potential $U = 0.5\ k\ (r - r_0)^2$ with $k/k_B = 96{,}500$ K/Å^2 and $r_0 = 1.54$ Å and a harmonic cosine bend potential $U = 0.5\ k\ (\cos\theta - \cos\theta_0)^2$ with $k/k_B = 62{,}500$ K/Å^2 and $\cos\theta_0 = 114°$. The interactions between guest molecules (hydrocarbons, sodium and calcium cations) and those between the guest molecules and the framework are modeled by Lennard-Jones and Coulombic potentials [14, 16, 21, 22]. The Lennard-Jones potentials are truncated at 12 Å and shifted so that the energy is zero at the cut-off distance.

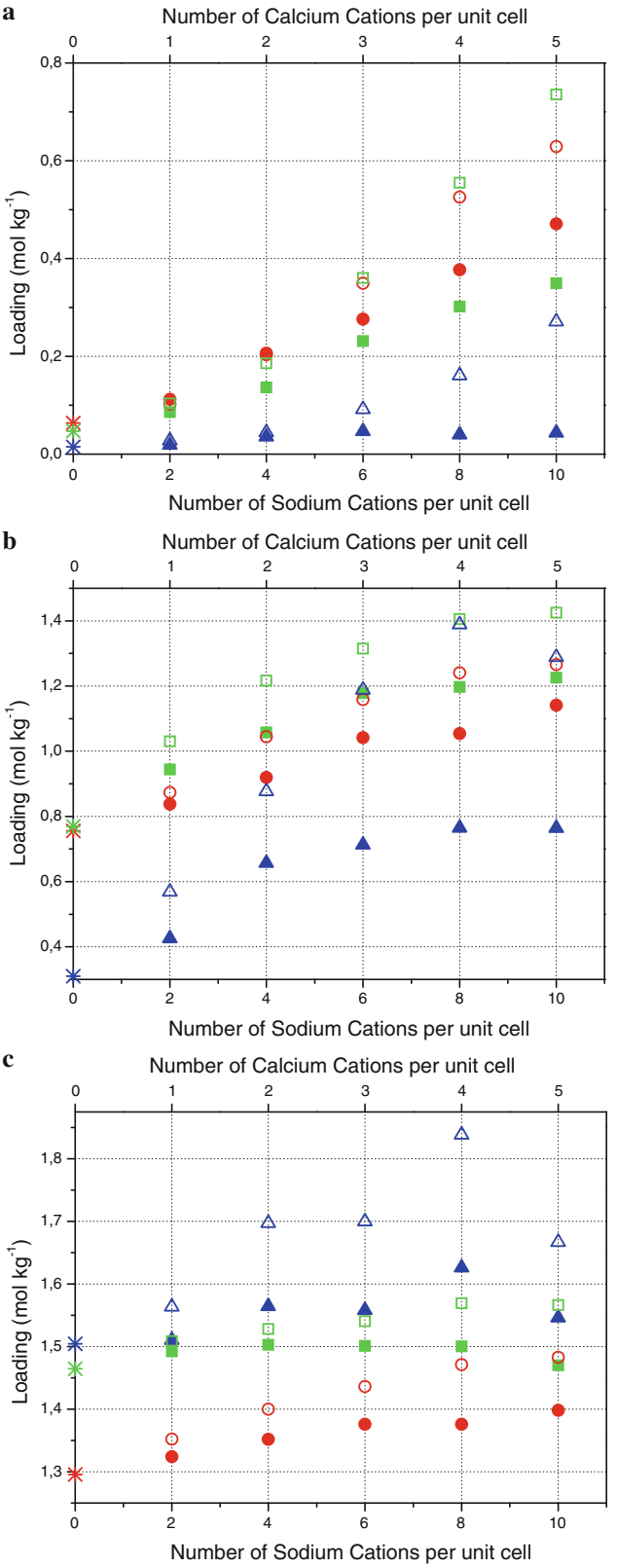

Fig. 3 Computed loading of hexane (*circles*), 3-methylpentane (*squares*) and 2,2-dimethylbutane (*triangles*) in polymorph A with Na (*open symbols*) and Ca cations (*solid symbols*) at 423 K and at **a** 0.1 kPa (*top*), **b** 2 kPa (*middle*) and **c** 27 kPa (*down*)

The Coulombic potentials were computed with Ewald summation technique, using a relative precision of 10^{-6}.

Periodic boundary conditions were applied in all directions. The number of unit cells in the simulation box was chosen such that the minimum length in each of the coordinate directions was larger than 24 Å. We use four units cells ($2 \times 2 \times 1$) for polymorph A ($a = b = 12.661$ Å, $c = 26.406$ Å) and eight units cells ($2 \times 2 \times 2$) for polymorph B ($a = 17.8965$ Å, $b = 17.92$ Å, $c = 14.3282$ Å). Polymorph A has orthorhombic symmetry while polymorph B is monoclinic with $\alpha = \gamma = 90°$ and $\beta = 114.803°$. The computed equipotential energy surfaces of the two polymorphs along the three axes are shown in Fig. 1. Simulations were performed for 22 structures, 11 for each polymorph, containing 0, 2, 4, 6, 8 and 10 sodium cations per unit cell or 1, 2, 3, 4 and 5 calcium cations per unit cell.

3 Results and discussion

Figure 2 shows the simulated adsorption isotherms of hexane, 3-methylpentane and 2,2-dimethylbutane in polymorphs A and B at 423 K. These simulations were performed for pure silica structures and compared with experimental isotherms measured by Barcia et al. [23] in commercial pellets of zeolite BEA at the same temperature. Such data are in fair agreement with pure component loadings in the Henry region, measured by Denayer et al. [24] in a laboratory-made BEA sample. Discrepancies between experimental and simulation data can be attributed to the structural differences between the simulated and the experimental structures. Adsorption loading is mainly affected by the faults at low pressures and by the pore volume at the higher pressures. The experimental pellets used by Barcia et al. [23] were 1/16 inch cylindrical extrudates of zeolite H-BEA with Si/Al ratio of 75 and an average length of 5 mm. The simulated polymorphs were defect-free crystal structures. The pore volume for this structure is 0.14 cm^3/g, and the apparent and the solid densities are 1.18 and 1.42 g/cm^3, respectively. Those values were measured by mercury porosimetry [6, 23, 25]. Compared to other zeolites, this structure has a high concentration of stacking defects that occur from the successive interconnection of layers in a given plane. On the contrary, the simulated polymorphs are free-defect crystals

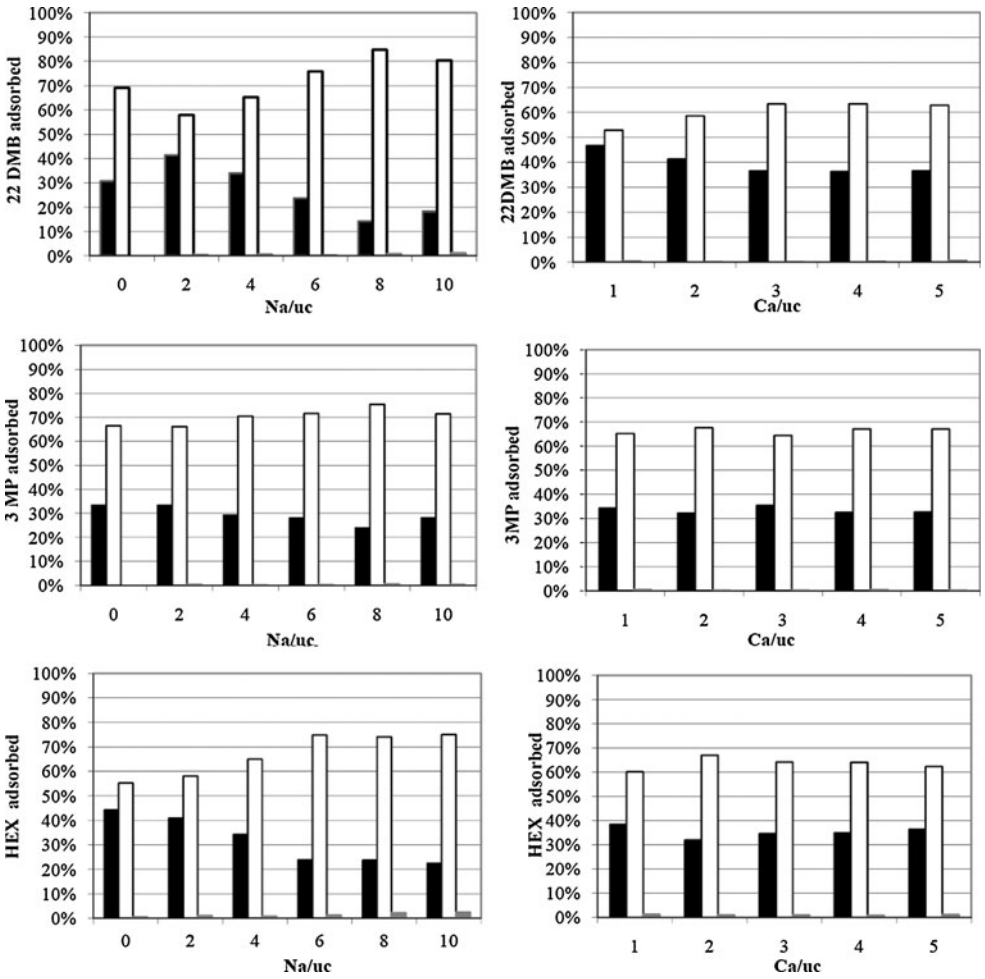

Fig. 4 Preferential adsorption sites obtained at 2 kPa and at 423 K for 2,2-dimethylbutane (*top*), 3-methylpentane (*middle*) and hexane (*bottom*) in the polymorph A containing sodium cations (*left*) and calcium cations (*right*). Straight channels (*black*), intersection channels (*white*) and zig–zag channels (*gray*)

with computed pore volumes 0.2763 cm^3/g (polymorph A) and 0.2721 cm^3/g (polymorph B) and with framework densities 1.508 g/cm^3 (polymorph A) and 1.530 g/cm^3 (polymorph B).

The computed adsorption loading of linear hexane, 3-methylpentane and 2,2-dimethylbutane in polymorph A as a function of the amount of aluminum framework atoms per unit cell and the type of non-framework cation is shown in Fig. 3 for 0.1 kPa (3a), 2 kPa (3b) and 27 kPa (3c). The simulations were performed at 423 K. In broad terms, the adsorption loading hierarchy is 3-methylpentane $\cong$ hexane $>$ 2,2-dimethylbutane at low pressures, 3-methylpentane $>$ hexane $>$ 2,2-dimethylbutane at medium pressures and 2,2-dimethylbutane $>$ 3-methylpentane $>$ hexane at high pressures. In addition, we observe an increase in adsorption loading with the amount of aluminum in the structure. The differences in adsorption between the structures with sodium and calcium cations enlarge with the amount of aluminum atoms in the structure; and for a given number of aluminum atoms, the adsorption loading is higher in the structure with sodium cations.

A more detailed observation in the low pressure regime (Fig. 3a) shows that the adsorption of 2,2-dimethylbutane is low and almost independent on the number of calcium cations, whereas it increases with the number of sodium cations. On the other hand, the number of cations highly influences the adsorption selectivity at this pressure. Hence, for a given number of aluminum atoms, the structure with sodium cations (i.e., number of sodium cations per unit cell equal to number of aluminum atoms per unit cell) favors 3-methylpentane adsorption, and the structure with calcium cations (i.e., number of calcium cations per unit cell half the number of aluminum atoms per unit cell) favors hexane adsorption. A similar inversion in selectivity is observed for hexane and 2,2-dimethylbutane at 2 kPa (Fig. 3b). The adsorption loading of hexane is higher than the adsorption for 2,2-dimethylbutane in the structures with calcium and in those with low density of sodium cations. However, the adsorption loading of hexane becomes similar or even lower than the adsorption for 2,2-dimethylbutane in the structures with a high density of sodium cations. At medium and high pressures, the structures with 8 aluminum atoms per unit cell show a maximum in the adsorption loading of 2,2-dimethylbutane. This maximum is wider for the structure with sodium cations.

To compute histograms with average occupation for the hexane isomers as well as for the two non-framework

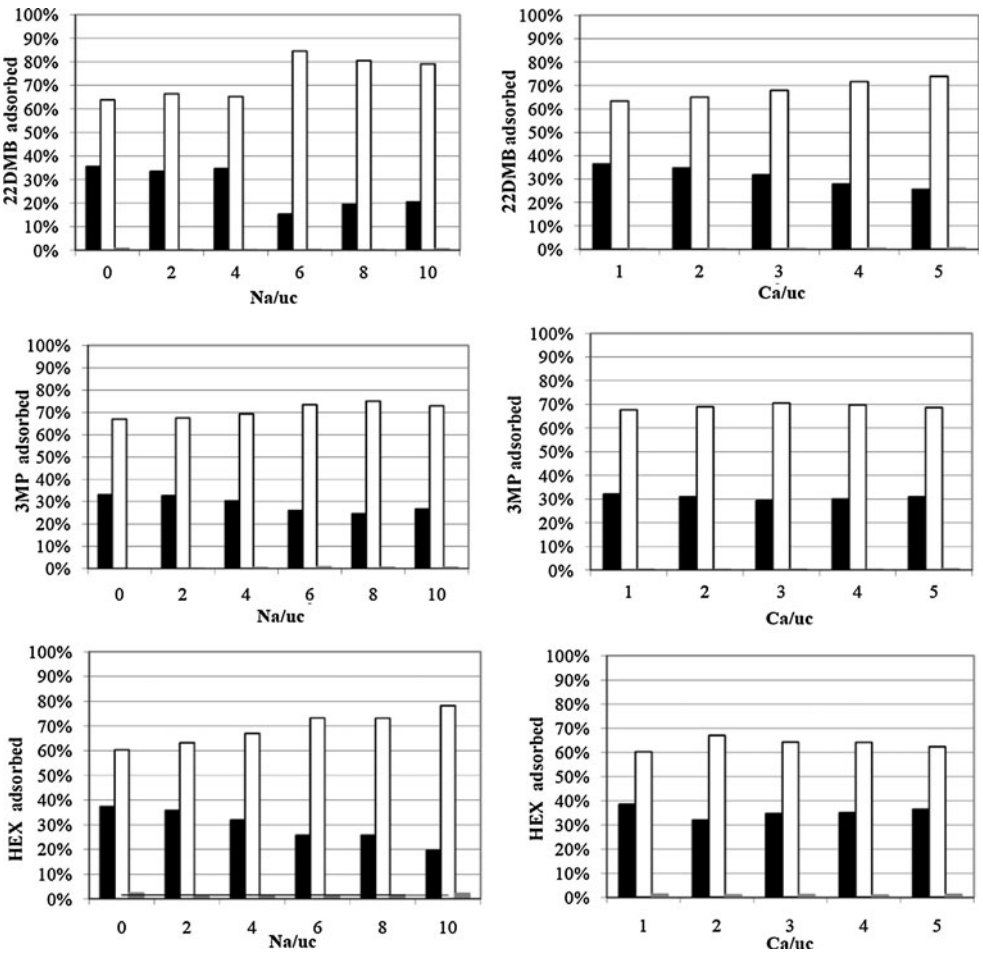

Fig. 5 Preferential adsorption sites obtained at 27 kPa and at 423 K for 2,2-dimethylbutane (*top*), 3-methylpentane (*middle*) and hexane (*bottom*) in the polymorph A containing sodium cations (*left*) and calcium cations (*right*). Straight channels (*black*), intersection channels (*white*) and zig–zag channels (*gray*)

cations, we have defined three adsorption sites: straight channels, intersection channels and zig–zag channels. The four vertical straight channels are located in regions of 1/3 unit cell in x and y direction. The height of each block is half a unit cell. The zig–zag channels are subparts of this block of z-length of 3% of a unit cell. Items are first checked to be within a zig–zag region. If not in there, they are checked to be in an intersection region (that corresponds to the bigger block). All atoms that are not located in either zig–zag or intersections are assumed to be in the straight channels.

The histograms with the average occupation for the hexane isomers are shown in Figs. 4 and 5 for 2 and 27 kPa, respectively. In general, the higher adsorption energy is found at the intersections, followed by the straight and the zig–zag channels. The amount of 2,2-dimethylbutane absorbed at the straight channels spans from 20 to 45%. The average occupation in the straight channel decreases with the amount of aluminum atoms per unit cell, reaching a maximum for the structures that contain 2 atoms of aluminum per unit cell. When the 2,2-dimethylbutane is adsorbed, both sodium and calcium cations are found preferentially at the straight channels (Figs. 6, 7), except for the structure with 2 aluminum atoms per unit cell, where the preferential location for the cations is the zig–zag channels.

The adsorption behavior of 3-methylpentane and hexane shows similar trends than for 2,2-dimethylbutane. Hence, the highest adsorption energy is observed at the intersections followed by the straight channels and a negligible amount in the zig–zag channels. As with the dibranched molecule, the percentage of occupation in the straight channels decreases for the highest amounts of aluminum framework atoms. This occupation is higher for hexane than for 3-methylpentane in the structures with sodium and low aluminum content (from 0 to 4 Al/uc) and reverses for the structures with the higher aluminum content (from 6 to 10 Al/uc). This behavior is not observed for the structures with calcium, where the straight channels show an occupation of 30–40% in all cases.

The preferential locations for the sodium and the straight channels, second the intersections and finally the zig–zag channels. The one exception to this hierarchy corresponds to the structures with two aluminum atoms per unit cell. At medium pressures (2 kPa), the preferential location of the two sodium cations per unit cell is at the zig–zag channels,

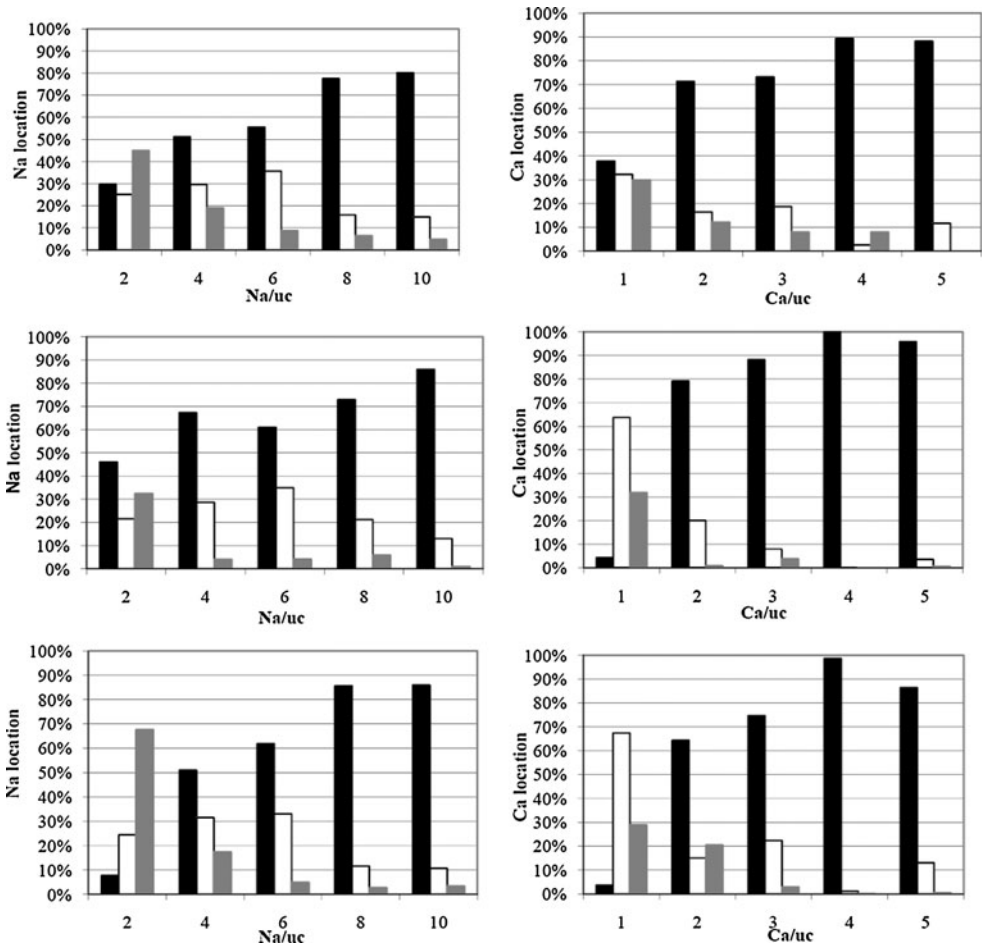

Fig. 6 Location of the non-framework cations at 2 kPa and at 423 K for polymorph A containing 2,2-dimethylbutane (*top*), 3-methylpentane (*middle*) and hexane (*bottom*). *Left*: sodium cations. *Right*: calcium cations. Straight channels (*black*), intersection channels (*white*) and zig–zag channels (*gray*)

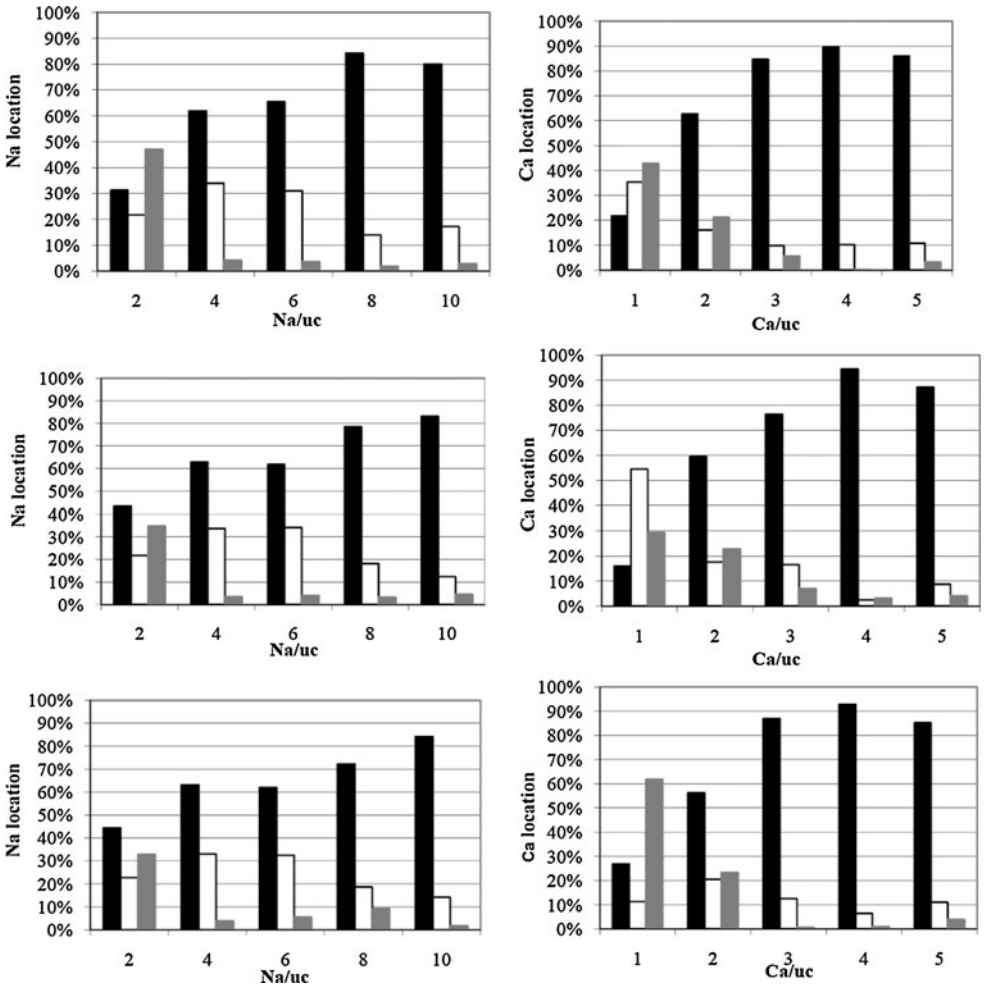

Fig. 7 Location of the non-framework cations at 27 kPa and at 423 K for polymorph A containing 2,2-dimethylbutane (*top*), 3-methylpentane (*middle*) and hexane (*bottom*). *Left*: sodium cations. *Right*: calcium cations. Straight channels (*black*), intersection channels (*white*) and zig–zag channels (*gray*)

followed by the straight channels for the structure containing branched alkanes and by the intersection channels for the structure containing hexane.

The preferential location of the calcium cation in the structures with 2 Al/uc depends on both the pressure and the type of alkane adsorbed in the structure. Hence, at medium pressures (2 kPa), the calcium cation is preferentially found at the intersections > zig–zag channels ≫ straight channels when the structure is loaded with hexane and 3-methylpentane and shows an almost homogeneous distribution between the three sites when the structure is loaded with 2,2-dimethylbutane. At higher pressures (27 kPa), the preferential locations of the calcium cations are the zig–zag channels followed by the intersections for the structure with 2,2-dimethylbutane, the zig–zag channels followed the straight channels for the structure with hexane and the intersections followed zig–zag channels for the structure with 3-methylpentane.

Figure 8 compares the loading obtained for the three isomers in polymorphs A and B at low (0.1 kPa), medium (2 kPa) and high pressures (27 kPa). The adsorption loading of hexane and the adsorption loading of 3-methylpentane and 2,2-dimethylbutane are almost independent of the polymorph used as well as of the type of non-framework cation contained in the structure. The only exception is for the dibranched alkane at 2 kPa. In this case, adsorption loading is slightly higher in the polymorph B, especially for the structures with the highest number of aluminum atoms per unit cell and with calcium as non-framework cation.

4 Conclusions

Configurational-bias Monte Carlo simulations have been used to analyze the adsorption behavior of hexane, 3-methylpentane and 2,2-dimethylbutane in the polymorphs A and B of zeolite BEA. The general observations and conclusions drawn from this work are that (1) the adsorption loading is almost independent of the polymorph used; (2) the linear and the monobranched alkanes are

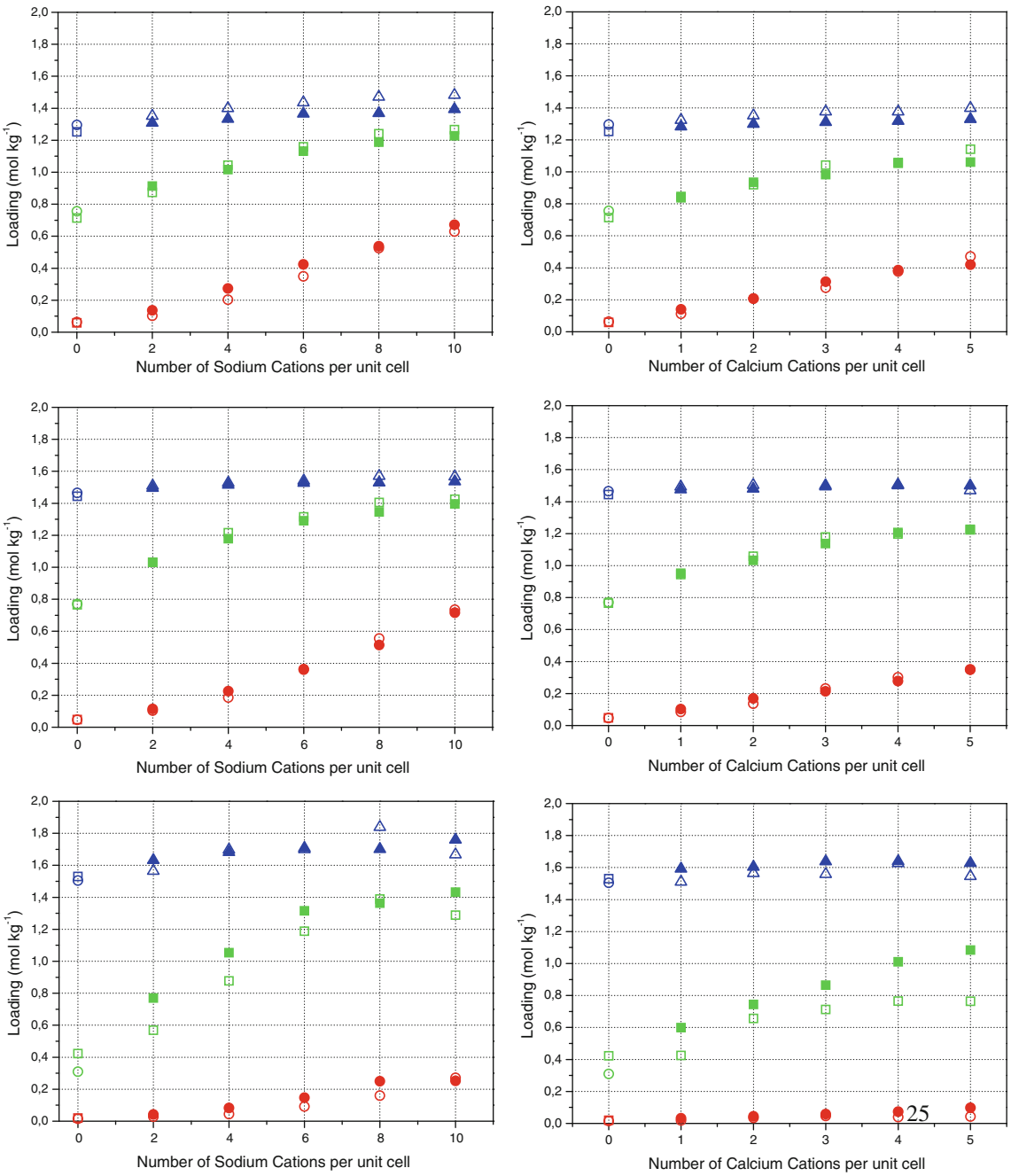

Fig. 8 Computed loading of hexane (*top*), 3-methylpentane (*middle*) and 2,2-dimethylbutane (*bottom*) at 0.1 kPa (*circles*), 2 kPa (*squares*) and 27 kPa (*triangles*) in polymorph A (*open symbols*) and B (*solid symbols*) for structures containing sodium non-framework cations (*left*) and structures containing calcium non-framework cations (*right*). Simulations were performed at 423 K

preferentially adsorbed in the structure at low and medium pressures, and the dibranched alkanes are adsorbed at the highest pressures; (3) differences in the adsorption loading between the structures with sodium and calcium cations enlarge when we increase the amount of aluminum framework atoms; (4) for a given number of aluminum atoms per unit cell, the adsorption loading is higher in the structure that contains sodium cations; and (5) the preferential adsorption sites are the intersections followed by the straight and the zig–zag channels.

Acknowledgments This work is supported by the Spanish "Ministerio de Educación y Ciencia (MEC)" (CTQ2007-63229), and Junta de Andalucía (P07-FQM-02595). E. García-Pérez, thanks the MEC for her predoctoral fellowship. We acknowledge J. M. Castillo for helpful suggestions and J. van Baten for providing data used in Figs. 4, 5, 6, and 7 and for critically reading the manuscript.

References

1. Wadlinger RL, Kerr GT, Rosinski EJ (1967) US Patent 3,308,069
2. Higgins JB et al (1988) Zeolites 8:446–452
3. Treacy MMJ, Newsam JM (1988) Nature 332:249–251
4. Huddersman K, Klimczyk M (1996) J Chem Soc Faraday Trans 92:143–147
5. Huddersman K, Klimczyk M (1996) Aiche J 42:405–408
6. Barcia PS, Silva JAC, Rodrigues AE (2007) Aiche J 53:1970–1981
7. Burke NR, Trimm DL, Howe RF (2003) Appl Catal B-Environ 46:97–104
8. Yoshimoto R et al (2007) J Phys Chem C 111:1474–1479
9. Kadgaonkar MD et al (2007) J Phys Chem C 111:9927–9935
10. Li PY, Tezel FH (2007) Microporous Mesoporous Mater 98:94–101
11. Lu LH et al (2007) Fluid Phase Equilibria 259:135–145
12. Liu H et al (2008) J Porous Mater 15:119–125
13. Baerlocher C, Meier WM, Olson DH (2001) Atlas of zeolite structure types. Elsevier, London
14. Calero S et al (2004) J Am Chem Soc 126:11377–11386
15. Garcia-Perez E et al (2007) Angewandte Chemie-Int Edn 46:276–278
16. Garcia-Perez E et al (2006) J Phys Chem B 110:23968–23976
17. Garcia-Perez E et al (2005) Appl Surf Sci 252:716–722
18. Garcia-Sanchez A et al (2007) Adsorpt Sci Technol 25:417–427
19. Liu B et al (2007) J Phys Chem C 111:10419–10426
20. Martin MG, Siepmann JI (1998) J Phys Chem B 102:2569–2577
21. Dubbeldam D et al (2004) Phys Rev Lett 93:
22. Dubbeldam D et al (2004) J Phys Chem B 108:12301–12313
23. Barcia PS, Silva JAC, Rodrigues AE (2005) Microporous Mesoporous Mater 79:145–163
24. Denayer JF et al (1998) J Phys Chem B 102:3077–3081
25. Barcia PS, Silva JAC, Rodrigues AE (2006) Ind Eng Chem Res 45:4316–4328